

Twisted mass Dirac spectrum

Krzysztof Cichy

Institut für Theoretische Physik, Goethe-Universität Frankfurt,

Max-von-Laue-Str. 1, 60438 Frankfurt am Main, Germany

Faculty of Physics, Adam Mickiewicz University,

Umultowska 85, 61-614 Poznań, Poland

K. Splittorff

Discovery Center, Niels Bohr Institute,

University of Copenhagen, Blegdamsvej 17,

DK-2100, Copenhagen Ø, Denmark

Savvas Zafeiropoulos

Jefferson Laboratory, 12000 Jefferson Avenue, Newport News, VA 23606, USA

Department of Physics, College of William and Mary,

Williamsburg, VA 23187-8795, USA

Institut für Theoretische Physik, Goethe-Universität Frankfurt,

Max-von-Laue-Str. 1, 60438 Frankfurt am Main, Germany

(Dated: December 5, 2016)

Abstract

The microscopic spectral density for lattice QCD with $N_f = 2 + 1 + 1$ twisted mass fermions is computed numerically and compared to analytical predictions of Wilson χ -PT at a fixed index. In this way, we obtain results for the chiral condensate and the low-energy constant W_8 .

I. INTRODUCTION

The systematic control and elimination of discretization errors has been the center of attention for the community of lattice field theories in the past decades. The twisted mass formulation of lattice QCD is one of the most successful ways to improve the cutoff effects of the Wilson discretization [1–3]. At maximal twist, the discretization errors in the action and the matrix elements are of $\mathcal{O}(a^2)$. The other main advantage of the twisted mass prescription is the absence of exceptional configurations, since the problem of small eigenvalues of the Hermitian Dirac operator is regulated by the addition of the twisted mass. This is therefore a very promising description which allows for fast simulations of dynamical fermions with solid theoretical foundations. The main drawback of this prescription is that parity and isospin symmetry are broken by cutoff effects of $\mathcal{O}(a^2)$. For a pedagogical and detailed introduction to the twisted mass formulation, we refer the reader to [4, 5]. Recently, the European Twisted Mass collaboration (ETMC) has been simulating twisted mass fermions at the physical pion mass [6, 7], which already gets rid of one extrapolation, namely the chiral one. However, physical point simulations come at a heavy price and simulations at a heavier pion mass are still performed. During the course of a lattice study, there is another necessary extrapolation to be made and it is the one to the continuum limit. When simulating closer and closer to the continuum limit, one faces extremely severe problems, mainly related to critical slowing down [8] and the freezing of topology. The introduction of open boundary conditions [9] significantly ameliorated the issue, but still simulations with values of the lattice spacing < 0.05 fm remain very difficult. So one needs to perform a combined chiral and continuum extrapolation and we advocate here for a lattice augmented version of the low energy Effective Field Theory (EFT) for QCD, which correctly incorporates discretization errors to leading order (LO) in a . The low-energy EFT for Wilson fermions, Wilson χ -PT, was introduced in [10–12]. It provides a systematic framework to study the quark mass dependence as well as the discretization effects in various, phenomenologically interesting observables. We refer the reader to [13] for a detailed and pedagogical introduction to Wilson χ -PT. Moreover, one can study the intricate phase diagram of twisted mass fermions in analytical mean field studies employing Wilson χ -PT [14–18]. When $m \propto a^2$, one has two possibilities, that of a second order phase transition to the so called Aoki phase [19] or a first order scenario (the Sharpe-Singleton scenario) [10]. The sign and the strength of the new

LECs which parametrize lattice artifacts determine which of the two scenarios is realized in practice during a lattice simulation, see e.g. [20]. By the same token, one can describe within Wilson χ -PT the changes in the orientation of the chiral condensate [13, 14, 18]. The chiral condensate changes promptly from -1 to +1 in the first order scenario, while it changes in a continuous manner in the Aoki phase. Finally, the extraction of the physical low energy constants, such as F_π and Σ , through fits to χ -PT formulae hinges strongly on the knowledge of the LECs of Wilson χ -PT. Consequently, there has been a great deal of analytical [21–30] and numerical [31–36] work on the extraction of the LECs of Wilson χ -PT. The LECs of Wilson χ -PT parametrize the pion mass splittings [32], the difference of the pion scattering lengths between channels with isospin zero and isospin equal to two [27, 33] and they also measure the departure from unitarity in a mixed action setup where one simulates overlap fermions in a sea of a cheaper discretization, e.g. twisted mass fermions [31].

A very promising method, which we will follow in this paper, is to extract the LECs of Wilson χ -PT by fitting analytical results derived in the framework of Wilson χ -PT in the ϵ -regime to eigenvalue densities of the Dirac operator computed on the lattice. We compute numerically the microscopic spectral density for lattice QCD with twisted mass fermions and compare it with the analytical result presented in [37]. We obtain results for the chiral condensate and the low-energy constant W_8 of Wilson χ -PT by fitting the lattice data for the microscopic spectral density of the Hermitian Wilson Dirac operator with a fixed index and at a finite volume to the analytical results. This is a case study at one value of the lattice spacing and at one volume, attempting, for the first time for dynamical twisted mass fermions, to study numerically the spectrum of the twisted mass Wilson Dirac operator, test the validity of the analytic results of Wilson χ -PT and extract directly from the spectrum two important low-energy constants. Preliminary results were presented in [38, 39].

II. THE THEORETICAL PRELUDE

A. Twisted mass QCD in the continuum

The fermionic part of the Lagrangian density of continuum twisted mass QCD, for two flavors, is given, in the twisted basis, by

$$\mathcal{L} = \bar{\chi}(\gamma_\mu D_\mu + m + iz_t \gamma_5 \tau_3)\chi, \quad (1)$$

where in addition to the usual Dirac term and the quark mass m , the so called twisted mass z_t has been introduced. Note that the twisted mass term has a non trivial Dirac and flavor structure, as it comes with τ_3 in flavor space and with γ_5 in Dirac space. The immediate consequence of the addition of this new mass term is that the determinant of the twisted mass Dirac operator D is strictly positive and one does not encounter the presence of the so-called exceptional configurations (these are configurations where the Dirac eigenvalue is almost equal to minus the quark mass and which correspond to an almost singular Dirac operator). This is achieved, since the spectrum of the Dirac operator is excluded by a strip of width $2z_t$ along the real axis [40], but can also immediately be seen by the fact that $\det(D + m + iz_t \gamma_5 \tau_3) = \det(D + m) \det((D + m)^\dagger) + z_t^2 > 0$. The connection of twisted mass to ordinary QCD is straightforward in the continuum if one considers the following chiral transformation [2],

$$\psi = \exp(i\omega \gamma_5 \tau_3/2)\chi, \quad \bar{\psi} = \bar{\chi} \exp(i\omega \gamma_5 \tau_3/2), \quad (2)$$

where $\omega = \arctan(z_t/m)$. Then, one can immediately rewrite the twisted mass Lagrangian density as

$$\mathcal{L} = \bar{\psi}(\gamma_\mu D_\mu + M)\psi, \quad (3)$$

where $M = \sqrt{m^2 + z_t^2}$ is the polar mass. The Grassmann fields ψ are in the physical basis. Since the transformation between the two bases is non-anomalous [2], one can consider it as merely a change of variables which relates twisted mass QCD to ordinary QCD. On the lattice, it was shown in [1] that this equivalence is still valid, but spoiled, as anticipated, by discretization errors.

B. Wilson χ -PT for twisted mass fermions

Entirely relying on symmetry properties, one can write down the chiral Lagrangian with $\mathcal{O}(a^2)$ terms included [10–12, 41]. In this study, we focus on the ϵ -regime, where $m \sim z_t \sim a^2 \sim 1/V$, and hence the pion Compton wavelength is much larger than the box where the

theory is regulated. Consequently, the partition function factorizes and is given by a zero dimensional unitary matrix integral describing the zero momentum modes [21–23, 25, 37, 42]. The partition function at a fixed vacuum angle θ is decomposed according to

$$Z_{N_f}(m, \theta; a) = \sum_{\nu=-\infty}^{\infty} e^{i\nu\theta} Z_{N_f}^{\nu}(m; a) \quad (4)$$

into an infinite sum of partition functions with a fixed index ν . The fixed index partition function for twisted mass fermions with all leading order (LO) in a discretization errors, in the ϵ -regime, reads

$$\begin{aligned} Z_{N_f}^{\nu}(m) = & \int_{U(N_f)} d\mu(U) \det^{\nu} U \exp \left[mV\Sigma \text{Tr} (U + U^{-1}) + zV\Sigma \text{Tr} \tau_3 (U - U^{\dagger}) \right] \\ & \times \exp \left[-a^2 V W_6 \text{Tr}^2 (U + U^{-1}) - a^2 V W_7 \text{Tr}^2 (U - U^{-1}) - a^2 V W_8 \text{Tr} (U^2 + U^{-2}) \right], \end{aligned} \quad (5)$$

where the complex matrix valued spurion fields m, a are taken to be real and proportional to the identity. As stated previously, ν is the index of Wilson Dirac operator (defined via the spectral flow lines [43–45]). Note that the partition function, apart from the chiral condensate Σ , involves three new unknown LECs $W_{6/7/8}$, which parametrize the discretization errors. Note that in this article, we follow the sign conventions of [37] which are the opposite of [12], where the same LECs are given by $-W'_{6/7/8}$, respectively. The values for the LECs $W_{6/7/8}$ are determined by the lattice action (e.g. a particular choice of the gauge action, improvement terms and/or the gauge field smearing in the Dirac operator, etc.) and can be determined through lattice simulations.

C. The microscopic spectral density for $N_f = 2$ twisted mass fermions

In [37], the microscopic spectral density of the Hermitian Dirac operator $D_5(m=0) \equiv \gamma_5 D(m=0)$ for a fixed index ν and two flavors at maximal twist was derived analytically. The authors of [37] employed the graded method, where one adds an additional fermionic quark and an additional bosonic (ghost) quark with twisted masses z and z' , respectively, to the partition function. This prescription is often referred to as partial quenching. In the approximation where $W_6 = W_7 = 0$, the supersymmetric partition function takes the form

$$Z_{3|1}^{\nu}(\mathcal{Z}; a) = \int_{Gl(3|1)/U(1)} d\mu(U) \text{Sdet}(iU)^{\nu} e^{\frac{i}{2} \text{Str}(\mathcal{Z}[U+U^{-1}]) + \hat{a}^2 \text{Str}(U^2 + U^{-2})}, \quad (6)$$

where \mathcal{Z} contains the appropriate sources with respect to which one differentiates in order to compute the desired spectral resolvent, see [37]. Here and below, we will use the notation $\widehat{m} = mV\Sigma$, $\widehat{z}_t = z_t V\Sigma$ and $\widehat{a}^2 = a^2 V W_8$. Neglecting $W_{6/7}$ is an approximation performed in order to simplify the analytical computation of the integral over the graded group $Gl(3|1)/U(1)$. It is also motivated by the conventional lore that the double-trace terms are suppressed in the large N_c limit [46].

Here, we will state the results from [37] needed in the present context. The spectral density can be computed through the discontinuity of the resolvent,

$$\rho_5^\nu(\widehat{\lambda}^5, \widehat{z}_t; \widehat{a}) = \left\langle \sum_k \delta(\widehat{\lambda}_k^5 - \widehat{\lambda}^5) \right\rangle_{N_f=2} = \frac{1}{\pi} \text{Im}[G_{3|1}^\nu(\widehat{z} = -\widehat{\lambda}^5, \widehat{z}_t; \widehat{a})]_{\epsilon \rightarrow 0}, \quad (7)$$

where $\widehat{\lambda}^5 = \lambda^5 V\Sigma$ are the rescaled eigenvalues of the Hermitian Wilson Dirac operator. After a lengthy and technical computation presented in [37], the final expression for the resolvent is

$$G_{3|1}^\nu(z, z_t; a) = G_{1|1}^\nu(z, z; a) + \frac{Z_2(iz_t, z; a)}{Z_2^\nu(iz_t, -iz_t; a)} \frac{z - iz_t}{2iz_t} G_{1|1}^\nu(-iz_t, z; a) - \frac{Z_2^\nu(-iz_t, z; a)}{Z_2^\nu(iz_t, -iz_t; a)} \frac{z + iz_t}{2iz_t} G_{1|1}^\nu(iz_t, z; a). \quad (8)$$

Where

$$G_{1|1}^\nu(z_1, z_2; a) = -\frac{1}{16a^2\pi} \int_{-\infty}^{\infty} ds dt \frac{1}{t + z_2 - is - z_1} e^{-(s^2+t^2)/(16a^2)} \times \left(\frac{is + z_1}{t + z_2} \right)^\nu Z_{1|1}^\nu(\sqrt{-(is + z_1)^2}, \sqrt{-(t + z_2)^2}, a = 0), \quad (9)$$

with

$$Z_{1|1}^\nu(m_1, m_2; a = 0) = \left(\frac{m_2}{m_1} \right)^\nu (I_\nu(m_1) m_2 K_{\nu+1}(m_2) + m_1 I_{\nu+1}(m_1) K_\nu(m_2)). \quad (10)$$

The remaining integrals are evaluated numerically in order to produce plots of the spectral density. In Figure 1 and 2, we plot the spectral density of the Hermitian twisted mass Wilson Dirac operator for the range of the parameters which are relevant to this study. In Figure 1, we plot the analytical result of the microscopic (ϵ -regime) spectral density for a fixed large value of the twisted mass for various values of the rescaled lattice spacing \widehat{a} for the three values of the index considered in this study ($|\nu| = 0, 1, 2$). In Figure 2, we plot the analytical result of the microscopic spectral density for a large fixed value of the rescaled lattice spacing for several values of the rescaled twisted mass.

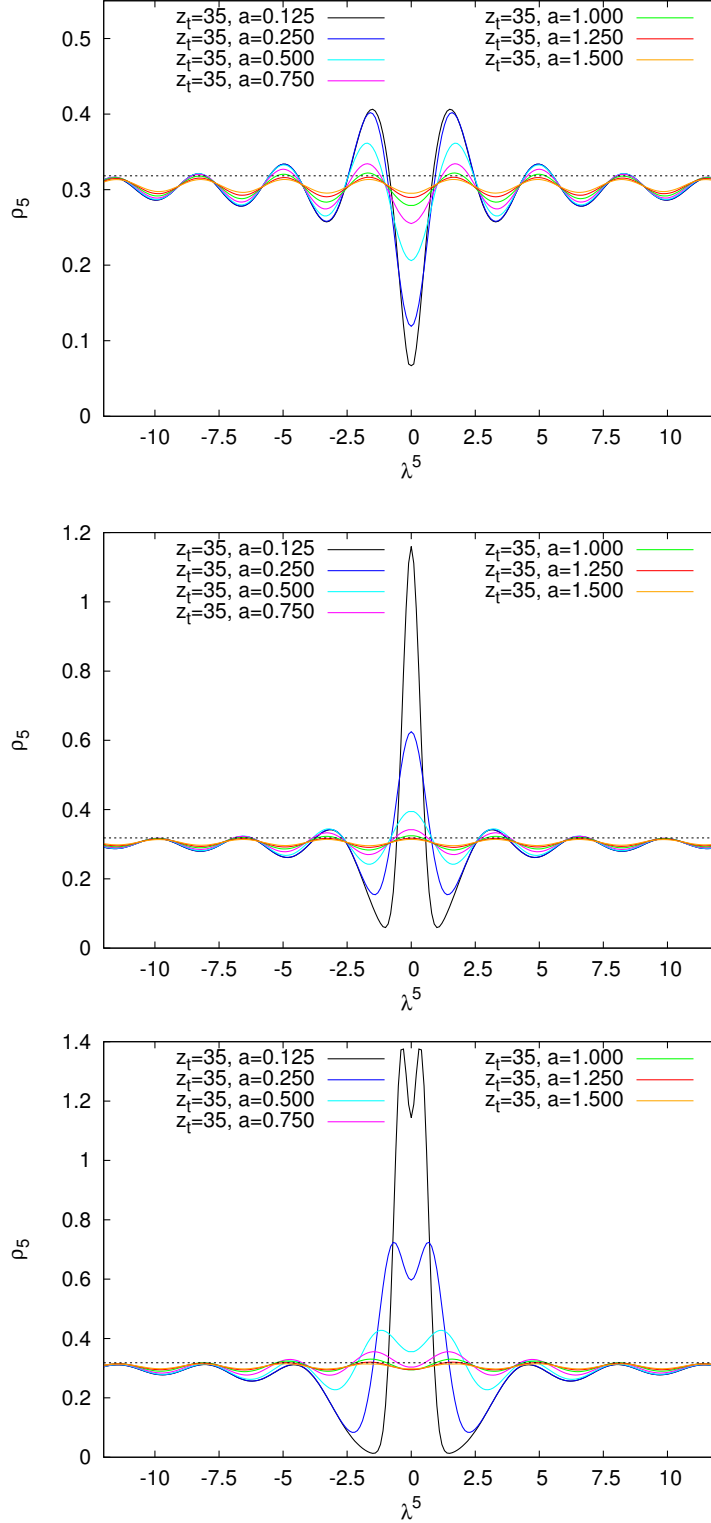


FIG. 1: The ϵ -regime spectral density of the Hermitian twisted mass Wilson Dirac operator is plotted for the lowest values of the topological charge ($|\nu| = 0, 1, 2$ in the first, second and third row, respectively). This is the analytical result derived in [37] plotted for $\hat{z}_t = 35$ and different values of the rescaled lattice spacing \hat{a} . Note that we have dropped the “hat” from the rescaled variables a , z_t in the legend of the plots.

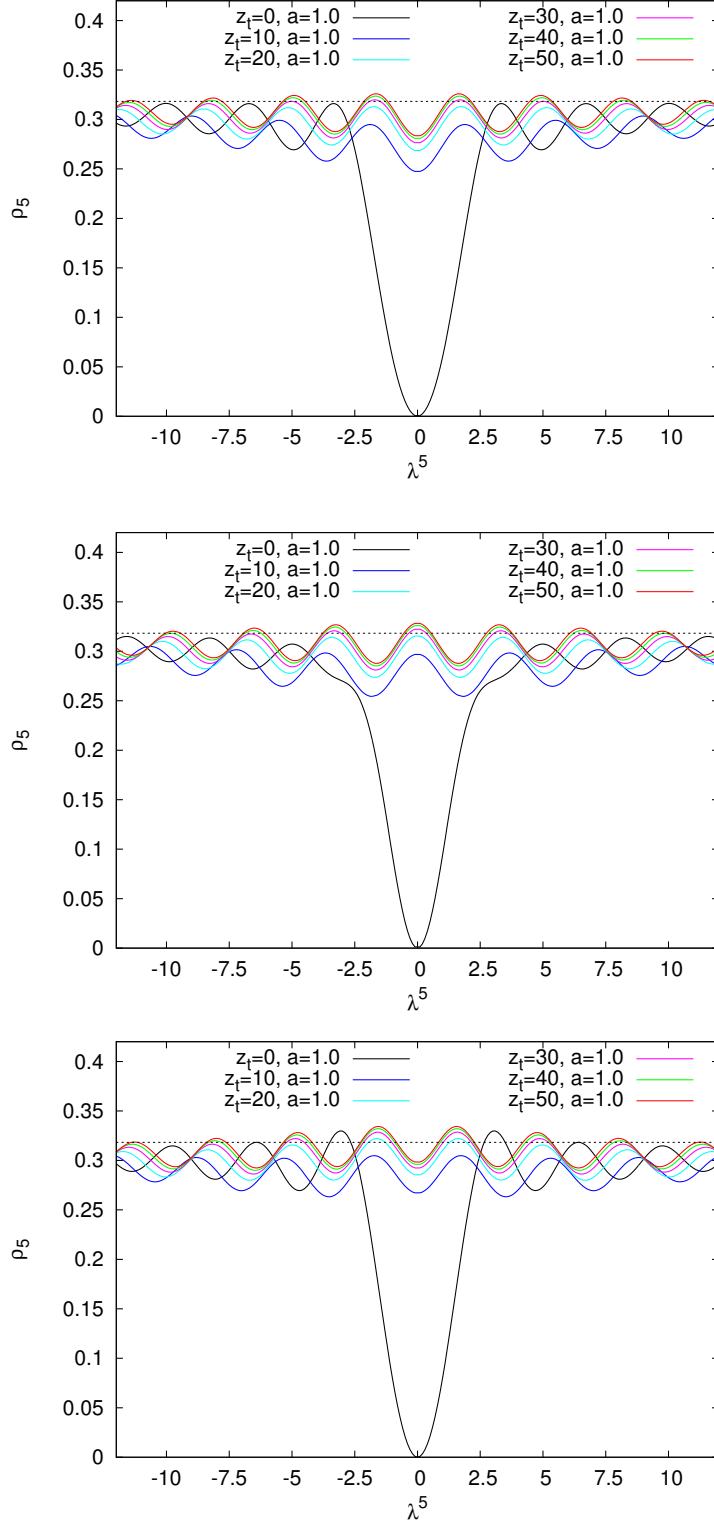


FIG. 2: As in Fig. 1, we plot here the ϵ -regime spectral density of the Hermitian twisted mass Wilson Dirac operator for $|\nu| = 0, 1, 2$ obtained in [37]. Here we have chosen $\hat{a} = 1$ and vary \hat{z}_t .

III. THE COMPUTATIONAL SETUP

A. The lattice action

In our study, we have been employing gauge field configurations with $N_f = 2 + 1 + 1$ dynamical twisted mass fermions at maximal twist. By courtesy of the European Twisted Mass Collaboration (ETMC), these are publicly available configurations [47, 48]. In the gauge sector, ETMC employs the Iwasaki action [49, 50], which is renormalization group improved and reads

$$S_{\text{gauge}} = \frac{\beta}{3} \sum_x \left(3.648 \sum_{\substack{\mu, \nu=1 \\ 1 \leq \mu < \nu}}^4 \{1 - \text{Re Tr}(U_{x, \mu, \nu}^{1 \times 1})\} - 0.331 \sum_{\substack{\mu, \nu=1 \\ \mu \neq \nu}}^4 \{1 - \text{Re Tr}(U_{x, \mu, \nu}^{1 \times 2})\} \right), \quad (11)$$

with β the inverse bare gauge coupling, $U_{x, \mu, \nu}^{1 \times 1}$ is the usual plaquette and $U_{x, \mu, \nu}^{1 \times 2}$ is the rectangular (1×2) Wilson loop. In the fermionic sector, we have two variants of the twisted mass action, one for the light degenerate u, d quarks and one for the heavy non-degenerate doublet of s, c quarks. The fermionic action for the degenerate light flavors reads [1–3]

$$S_{\text{light}}[\chi, \bar{\chi}, U] = \sum_x \bar{\chi}_l(x) [D_W + m_{(0,l)} + i\gamma_5 \tau_3 \mu_l] \chi_l(x), \quad (12)$$

where $m_{(0,l)}$ is the untwisted bare light quark mass, μ_l is the bare twisted mass in the light sector. For the heavy non-degenerate strange and charm quarks, we have [3, 51]

$$S_{\text{heavy}}[\chi, \bar{\chi}, U] = a^4 \sum_x \{ \bar{\chi}_h(x) [D[U] + m_{(0,h)} + i\mu_\sigma \gamma_5 \tau_1 + \mu_\delta \tau_3] \chi_h(x) \}, \quad (13)$$

where $m_{(0,h)}$ is the untwisted bare quark mass for the heavy doublet, μ_σ the bare twisted mass of the heavy doublet. Note that the twist angle is this time along the τ_1 direction and μ_δ the mass splitting along the τ_3 direction. The Wilson Dirac operator D_W is defined through the addition of the lattice Laplacian to the naive symmetric covariant derivative

$$D_W = \frac{1}{2} \gamma_\mu (\nabla_\mu + \nabla_\mu^*) - \frac{a}{2} \nabla_\mu^* \nabla_\mu, \quad (14)$$

where ∇_μ and ∇_μ^* denote the forward and backward covariant derivatives.

This study employs one lattice ensemble with lattice spacing $a = 0.0815(30)$ fm [52], the lattice volume is $32^3 \times 64$, the physical extent of the box is $L \sim 2.5$ fm and the bare twisted

masses are equal to $a\mu_l = 0.0055$, $a\mu_\sigma = 0.135$ and $a\mu_\delta = 0.170$. The pion mass computed from these configurations is equal to around 370 MeV. The quite large physical extent of the box takes care of the finite volume corrections, which are $\mathcal{O}(e^{-m_\pi L})$, and $m_\pi L \approx 5$ for our setup. Even though the pion mass in this simulation does not satisfy $1/M_\pi \gg L$, the smallest eigenvalues can be in the ϵ -regime. The characteristic energy scale below which the Dirac eigenvalues are described by the ϵ -regime of Wilson χ -PT is called, in an analogy to the condensed matter literature, the Thouless energy [53].

B. The computation of the index

The integer ν in Wilson χ -PT is the index of the Wilson Dirac operator. The direct numerical computation of the index of the Wilson Dirac operator is quite demanding. In our study, we have therefore utilized a gluonic definition of the topological charge combined with smearing via the Wilson flow [54]. The Wilson flow is an economical method, with solid theoretical foundations. Another attractive feature of it is that it does not involve additive or multiplicative renormalization. In order to test the sensitivity to the used method, we have employed various discretizations of the topological charge density. The first discretization as mentioned, utilizes the Wilson plaquette definition and has discretization errors of $\mathcal{O}(a^2)$ [55], the second definition includes the addition of the clover term and has discretization errors of $\mathcal{O}(a^2)$ [55]. The third discretization has rectangular clover terms and has discretization errors of $\mathcal{O}(a^4)$ [55]. The agreement and correlation among these three methods for the given value of the lattice spacing is above 98%, see [56] for a more detailed analysis.

C. Numerical results and the extraction of Σ and W_8

As demonstrated in Figure 1 and 2, the smallest eigenvalues of the Hermitian Wilson Dirac operator at a fixed topological sector are sensitive to the LECs of Wilson χ -PT. We therefore compute the lowest eigenvalues of the massless Hermitian Dirac operator at a fixed index. In order to obtain results with controlled statistical errors, we employed the B55.32 ensemble, which is one of the longest ensembles of the ETMC. This ensemble has $2 + 1 + 1$ flavors, but the heavy charm and strange quarks, whose bare twisted masses ($a\mu_s = 0.0158$ and $a\mu_c = 0.2542$) are much larger than the smallest Dirac eigenvalues, behave

as quenched from the point of view of the Dirac spectrum. This allows us to compare with the analytical results of the spectral density with $N_f = 2$. Starting with 5000 independent configurations, we measured the topological charge and computed the lowest eigenvalues of the Dirac operator for the sectors with index $|\nu| = 0, 1, 2$.

In Figure 3, we present the comparison of the analytical results of RMT vs. histograms of lattice data for the microscopic spectral density ρ^5 of the Hermitian Wilson Dirac operator D_5 in the sectors with $|\nu| = 0, 1, 2$. The error bars of the lattice data correspond to statistical errors computed with the bootstrap method. We see that the restricted number of gauge configurations in the sectors with $|\nu| = 0, 1, 2$ leads to quite large statistical uncertainties. This is natural, since for this large physical volume, the fluctuation of the topological charge is quite large. We started with a total of 5000 gauge configurations, but out of them only ~ 200 have $\nu = 0$, then ~ 400 have $|\nu| = 1$ and also ~ 400 have $|\nu| = 2$. In Figure 3, we immediately see that the dimensionless rescaled parameters \hat{z}_t and \hat{a} correspond to rather large values and this results in quite flat distributions. Due to the large value of \hat{a} , the peaks which correspond to the zero modes of the continuum theory have been completely depleted, as we observe in the middle and lower plot of Figure 3, which correspond to $|\nu| = 1, 2$, respectively.

The extraction of the LECs Σ and W_8 ($W_6 = W_7 = 0$ in the analytical formulae) was performed through fits with \hat{z}_t and \hat{a} as fitting parameters. In all cases, we obtain fits with $\chi^2/\text{d.o.f.} < 1$. Once \hat{z}_t and \hat{a} have been determined from the best fit, one can obtain Σ and W_8 through the definition of the scaling variables. We observe that there are some differences in the numerical values extracted from the different topological sectors.

The bare condensate values extracted from the matching of the analytical formulae to the lattice data require multiplicative renormalization. For the case of twisted mass fermions, the relevant renormalization constant is Z_P (contrasted to Z_S for ordinary untwisted Wilson fermions). Z_P was computed for these values of the parameters by the ETMC in [52, 57, 58] and it was found to be, in the \overline{MS} scheme at 2 GeV, $Z_P = 0.509(4)$ (we use the value from [52]). The renormalized values of Σ that appear in Table I are in quite good agreement with the results computed by ETMC with the method of spectral projectors in [59], where Σ in the continuum limit was found to be, translated to physical units, $\Sigma^{1/3} \approx 290 \pm 11$ MeV. The quite good agreement is very encouraging and indicates that discretization errors are taken into account to a certain degree by matching lattice results to LO Wilson χ -PT

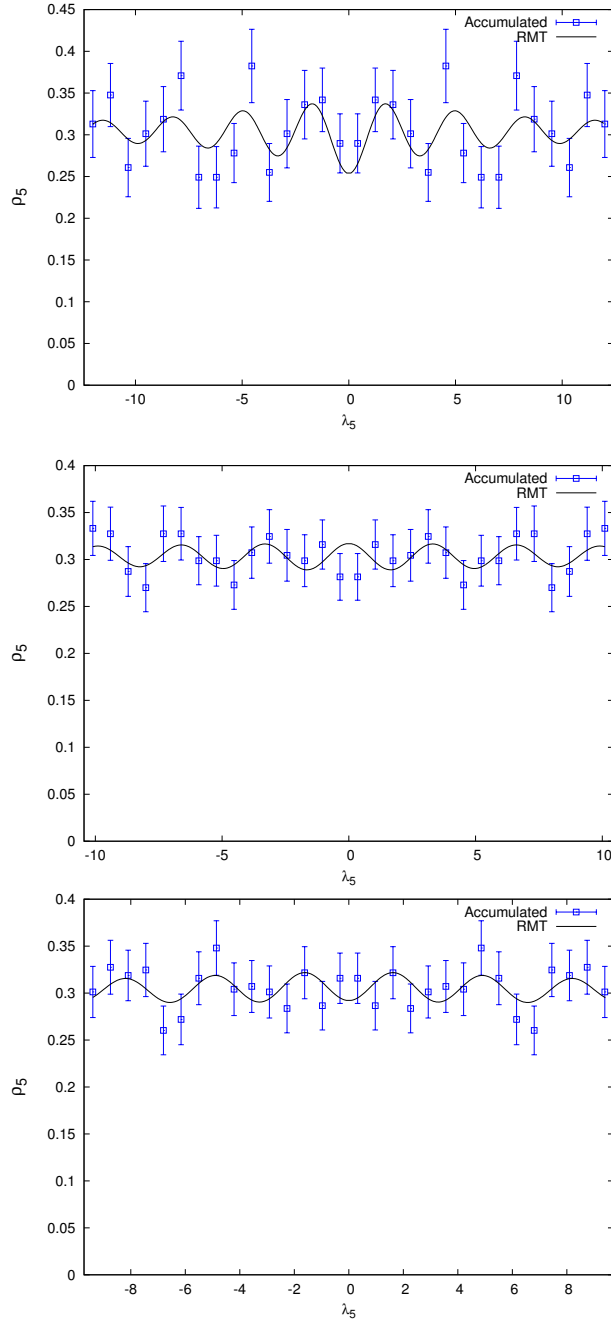


FIG. 3: The ϵ -regime spectral density of the Hermitian twisted mass Wilson Dirac operator is plotted for the lowest values of the index. The solid curves are fits of the analytical results derived in [37] to the data points, which are the numerical results from a lattice simulation on a $32^3 \times 64$ lattice with a lattice spacing $a = 0.0815$ fm and twisted mass $a\mu = 0.0055$. The top plot contains the fitting results of the topological sector with $\nu = 0$, where the values of the fitting parameters are given by $\hat{z}_t = 37.4(3.0)(0.5)$ and $\hat{a} = 0.78(27)(12)$. In the middle, the results for $|\nu| = 1$ are plotted with fitting parameters $\hat{z}_t = 32.4(2.5)(0.4)$ and $\hat{a} = 1.22(29)(14)$, finally in the bottom, we show the results for $|\nu| = 2$, where the fitting parameters are given by $\hat{z}_t = 31.3(4.1)(1.7)$ and $\hat{a} = 1.18(28)(9)$. In all the quoted values of \hat{z}_t and \hat{a} , the first error is the statistical one, while the second is a systematic one originating from the comparison of different bin sizes.

$ \nu $	0	1	2
$\Sigma^{1/3}$ [MeV]	285.9(8.6)(1.3)	272.5(6.6)(1.1)	269.2(11.0)(4.7)
W_8 [$r_0^6 W_0^2$]	0.0030(23)(10)	0.0069(32)(16)	0.0065(31)(10)

TABLE I: Extracted values for Σ and W_8 . In all the quoted values, the first error is statistical, while the second one is systematic originating from the comparison of different bin sizes.

which only includes the single trace term, i.e. the one proportional to W_8 . At this point, it is important to say that the only real way to check this is via the analytical computation of the microscopic spectral density containing the two double trace terms, since then the residual dependence would be of $\mathcal{O}(a^4)$, and to compare the change on the extracted values of Σ . The value that we extract for W_8 is in agreement with the mixed action studies [31], but differs by roughly a factor of 2 from the one determined in [32].

Here, some more comments regarding the fitting procedure are in order. It is clear that the approximation of neglecting the terms proportional to W_6 and W_7 in the chiral Lagrangian can only be justified in the large- N_c limit, where single trace terms dominate. This is by far not the case here and this can only be treated as an approximation that simplifies the cumbersome analytical solution. In [25], the exact analytical dependence on W_6 and W_7 was studied for all the different eigenvalue densities (complex, real) of the unimproved non-Hermitian Wilson Dirac operator. In Fig. 1 of [25], the effect of these LECs is described schematically. What was observed was that W_6 leads to a broadening of the Dirac spectrum parallel to the real axis according to a Gaussian with a width proportional to $\hat{a}_6 = \sqrt{V W_6} a$. Also W_7 has a non-trivial effect on the spectrum of the unimproved Wilson Dirac operator and once $W_6 = 0$, the purely imaginary eigenvalues enter the real axis via the origin, while the real eigenvalues are broadened by a Gaussian with a width proportional to $\hat{a}_7 = \sqrt{V W_7} a$. In order to take into account this effect, we allow for a free normalization in the x -axis, since this accounts to a certain extent for this broadening or squeezing of the spectrum due to W_6 and W_7 . When everything is properly taken into consideration, the locations of the peaks of the spectral density correspond to single eigenvalue distributions and therefore it is clear that lattice and analytical data have to perfectly agree on the location of the peaks.

For the case of $\nu = 0$, we performed a comparison of a free normalization parameter (multiplying the eigenvalues λ^5 entering the fitting ansatz) and of no extra rescaling. With an

extra multiplicative normalization (fitted to be $1.08(14)(2)$), we obtained $z_t = 37.4(3.0)(0.5)$ and $\hat{a} = 0.78(27)(12)$, which leads to $\Sigma = 285.9(8.6)(1.3)$ MeV and $W_8 = 0.0030(23)(10)$. For the case of no multiplicative normalization, we obtained $z_t = 39.2(9)(3)$ and $\hat{a} = 0.75(24)(13)$, which yields $\Sigma = 290.5(2.3)(0.8)$ MeV and $W_8 = 0.0027(19)(12)$, i.e. a result compatible with the one without the normalization. For non-trivial topological sectors, fits without the normalization fail to describe the data completely. The values of the normalization constant for $|\nu| = 1, 2$ were obtained as: $1.27(9)(2)$ and $1.29(14)(6)$, respectively. This further motivates (apart from the theoretical arguments given above) the derivation of analytical formulae including W_6 and W_7 . It is important to point out, that one could naively think that the low energy constant W_7 drops out for the case of $N_f = 2$ due to the properties of $SU(2)$ matrices ($(\text{Tr}U)^2 = \text{Tr}U^2 + 2$) and thus, one needs to care only about the LEC W_6 which can actually be combined with W_8 to one LEC $c_2 = W_6 + W_8/2$. However, despite the fact that this is true for the partition function itself, it is not true for the spectral density, which is actually computed via the supersymmetric $\mathcal{Z}_{3/1}$ generating function.

IV. CONCLUSIONS

In this article, we made the first attempt to compute the microscopic spectral density of twisted mass fermions via a direct lattice simulation. The ultimate goal was to validate analytical predictions of Wilson Chiral Perturbation Theory and to check the feasibility of the extraction of the chiral condensate Σ and the W_8 , which are two LECs of the chiral Lagrangian. This study was performed within the approximation that the other two LECs W_6 and W_7 , which also appear at leading order in a^2 , are set to zero. We plan to check the validity of this assumption in an upcoming publication after we first extend the analytical result of [37] to include the effects described by the double trace terms (the ones involving W_6 and W_7). The extraction of the chiral condensate Σ is rather robust, since this is mainly controlled by the “height” of the microscopic eigenvalue density, which we could determine fairly unambiguously and our findings are in reasonable agreement with the existing literature. However, the extraction of W_8 has proven to be an ordeal for almost all lattice approaches. In our study, this is quite a difficult task mainly due to the fact that for large values of \hat{a} , the microscopic spectral density becomes less dependent on the value of \hat{a} . A similar effect has been analytically shown for the microscopic eigenvalue density of the

unimproved Wilson Dirac operator, cf. Fig. 5 of [25]. For this aspect, simulations at a finer lattice spacing would be very helpful.

V. ACKNOWLEDGEMENTS

This study was based on a variant of the ETM collaboration’s public lattice Quantum Chromodynamics code, tmLQCD [60, 61]. We would like to thank Elena Garcia-Ramos, Gregorio Herdoiza, Karl Jansen, Mario Kieburg, Joyce C. Myers and in particular Jac Verbaarschot for fruitful discussions and Andreas Athenodorou for providing us with the data of the topological charge. This work was granted access to the HPC resources of CINES and IDRIS under the allocations offered by GENCI. We express our gratitude to the staff of this Computing facility for their constant help. This work was supported by the the Humboldt Foundation, the National Science Foundation (USA) under grant PHY-1516509 (S.Z.) and the Sapere Aude program of The Danish Council for Independent Research (K.S.). K.C. was supported in part by the Deutsche Forschungsgemeinschaft (DFG), project nr. CI 236/1-1.

-
- [1] R. Frezzotti *et al.* [Alpha Collaboration], “Lattice QCD with a chirally twisted mass term,” JHEP **0108**, 058 (2001) [hep-lat/0101001].
 - [2] R. Frezzotti and G. C. Rossi, “Chirally improving Wilson fermions. 1. O(a) improvement,” JHEP **0408**, 007 (2004) [hep-lat/0306014].
 - [3] R. Frezzotti and G. C. Rossi, “Chirally improving Wilson fermions. II. Four-quark operators,” JHEP **0410**, 070 (2004) [hep-lat/0407002].
 - [4] S. Sint, “Lattice QCD with a chiral twist,” hep-lat/0702008.
 - [5] A. Shindler, “Twisted mass lattice QCD,” Phys. Rept. **461**, 37 (2008) [arXiv:0707.4093 [hep-lat]].
 - [6] A. Abdel-Rehim *et al.*, “Nucleon and pion structure with lattice QCD simulations at physical value of the pion mass,” Phys. Rev. D **92**, no. 11, 114513 (2015) Erratum: [Phys. Rev. D **93**, no. 3, 039904 (2016)] [arXiv:1507.04936 [hep-lat]].
 - [7] A. Abdel-Rehim *et al.* [ETM Collaboration], “Simulating QCD at the Physical Point with $N_f = 2$ Wilson Twisted Mass Fermions at Maximal Twist,” arXiv:1507.05068 [hep-lat].

- [8] S. Schaefer *et al.* [ALPHA Collaboration], “Critical slowing down and error analysis in lattice QCD simulations,” Nucl. Phys. B **845**, 93 (2011) [arXiv:1009.5228 [hep-lat]].
- [9] M. Luscher and S. Schaefer, “Lattice QCD without topology barriers,” JHEP **1107**, 036 (2011) [arXiv:1105.4749 [hep-lat]].
- [10] S. R. Sharpe and R. L. Singleton, Jr, “Spontaneous flavor and parity breaking with Wilson fermions,” Phys. Rev. D **58**, 074501 (1998) [hep-lat/9804028].
- [11] G. Rupak and N. Shoresh, “Chiral perturbation theory for the Wilson lattice action,” Phys. Rev. D **66**, 054503 (2002) [hep-lat/0201019].
- [12] O. Bar, G. Rupak and N. Shoresh, “Chiral perturbation theory at $O(a^2)$ for lattice QCD,” Phys. Rev. D **70**, 034508 (2004) [hep-lat/0306021].
- [13] S. R. Sharpe, “Applications of Chiral Perturbation theory to lattice QCD,” hep-lat/0607016.
- [14] S. R. Sharpe and J. M. S. Wu, “The Phase diagram of twisted mass lattice QCD,” Phys. Rev. D **70**, 094029 (2004) [hep-lat/0407025].
S. R. Sharpe and J. M. S. Wu, “Applying chiral perturbation to twisted mass lattice QCD,” Nucl. Phys. Proc. Suppl. **140**, 323 (2005) [hep-lat/0407035].
- [15] L. Scorzato, “Pion mass splitting and phase structure in twisted mass QCD,” Eur. Phys. J. C **37**, 445 (2004) [hep-lat/0407023].
- [16] G. Munster, “On the phase structure of twisted mass lattice QCD,” JHEP **0409**, 035 (2004) [hep-lat/0407006].
- [17] M. Kieburg, K. Splittorff, J. J. M. Verbaarschot and S. Zafeiropoulos, “Phase Diagram of Wilson and Twisted Mass Fermions at finite isospin chemical potential,” PoS LATTICE **2014**, 065 (2015) [arXiv:1411.2570 [hep-lat]].
- [18] O. Janssen, M. Kieburg, K. Splittorff, J. J. M. Verbaarschot and S. Zafeiropoulos, “Phase Diagram of Dynamical Twisted Mass Wilson Fermions at Finite Isospin Chemical Potential,” Phys. Rev. D **93** (2016) no.9, 094502 [arXiv:1509.02760 [hep-lat]].
- [19] S. Aoki, “New Phase Structure for Lattice QCD with Wilson Fermions,” Phys. Rev. D **30**, 2653 (1984).
- [20] M. Kieburg, K. Splittorff and J. J. M. Verbaarschot, “The Realization of the Sharpe-Singleton Scenario,” Phys. Rev. D **85**, 094011 (2012) [arXiv:1202.0620 [hep-lat]].
- [21] P. H. Damgaard, K. Splittorff and J. J. M. Verbaarschot, “Microscopic Spectrum of the Wilson Dirac Operator,” Phys. Rev. Lett. **105**, 162002 (2010) [arXiv:1001.2937 [hep-th]].

- [22] G. Akemann, P. H. Damgaard, K. Splittorff and J. J. M. Verbaarschot, “Spectrum of the Wilson Dirac Operator at Finite Lattice Spacings,” *Phys. Rev. D* **83**, 085014 (2011) [arXiv:1012.0752 [hep-lat]].
- [23] M. Kieburg, J. J. M. Verbaarschot and S. Zafeiropoulos, “Eigenvalue Density of the non-Hermitian Wilson Dirac Operator,” *Phys. Rev. Lett.* **108**, 022001 (2012) [arXiv:1109.0656 [hep-lat]].
- [24] M. T. Hansen and S. R. Sharpe, “Constraint on the Low Energy Constants of Wilson Chiral Perturbation Theory,” *Phys. Rev. D* **85**, 014503 (2012) [arXiv:1111.2404 [hep-lat]].
- [25] M. Kieburg, J. J. M. Verbaarschot and S. Zafeiropoulos, “Spectral Properties of the Wilson Dirac Operator and random matrix theory,” *Phys. Rev. D* **88**, 094502 (2013) [arXiv:1307.7251 [hep-lat]].
- [26] M. Kieburg, J. J. M. Verbaarschot and S. Zafeiropoulos, “Dirac Spectrum of the Wilson Dirac Operator for QCD with Two Colors,” *Phys. Rev. D* **92**, no. 4, 045026 (2015) [arXiv:1505.01784 [hep-lat]].
- [27] S. Aoki, O. Bar and B. Biedermann, “Pion scattering in Wilson chiral perturbation theory,” *Phys. Rev. D* **78**, 114501 (2008) [arXiv:0806.4863 [hep-lat]].
- [28] O. Bar, S. Necco and A. Shindler, *JHEP* **1004**, 053 (2010) doi:10.1007/JHEP04(2010)053 [arXiv:1002.1582 [hep-lat]].
- [29] O. Bar, S. Necco and S. Schaefer, *JHEP* **0903**, 006 (2009) doi:10.1088/1126-6708/2009/03/006 [arXiv:0812.2403 [hep-lat]].
- [30] O. Bär and B. Hörz, *Phys. Rev. D* **90**, no. 3, 034508 (2014) doi:10.1103/PhysRevD.90.034508 [arXiv:1402.6145 [hep-lat]].
- [31] K. Cichy, V. Drach, E. Garcia-Ramos, G. Herdoiza and K. Jansen, “Overlap valence quarks on a twisted mass sea: a case study for mixed action Lattice QCD,” *Nucl. Phys. B* **869**, 131 (2013) [arXiv:1211.1605 [hep-lat]].
- [32] G. Herdoiza, K. Jansen, C. Michael, K. Ottnad and C. Urbach, “Determination of Low-Energy Constants of Wilson Chiral Perturbation Theory,” *JHEP* **1305**, 038 (2013) [arXiv:1303.3516 [hep-lat]].
- [33] F. Bernardoni, J. Bulava and R. Sommer, “Determination of the Wilson ChPT low energy constant c_2 ,” *PoS LATTICE* **2011**, 095 (2011) [arXiv:1111.4351 [hep-lat]].
- [34] P. H. Damgaard, U. M. Heller and K. Splittorff, “Finite-Volume Scaling of the Wilson Dirac

- Operator Spectrum,” Phys. Rev. D **85**, 014505 (2012) [arXiv:1110.2851 [hep-lat]].
- [35] A. Deuzeman, U. Wenger and J. Wuilloud, “Spectral properties of the Wilson Dirac operator in the ϵ -regime,” JHEP **1112**, 109 (2011) [arXiv:1110.4002 [hep-lat]].
 - [36] P. H. Damgaard, U. M. Heller and K. Splittorff, “New Ways to Determine Low-Energy Constants with Wilson Fermions,” Phys. Rev. D **86**, 094502 (2012) [arXiv:1206.4786 [hep-lat]].
 - [37] K. Splittorff and J. J. M. Verbaarschot, “The Microscopic Twisted Mass Dirac Spectrum,” Phys. Rev. D **85**, 105008 (2012) [arXiv:1201.1361 [hep-lat]].
 - [38] K. Cichy, E. Garcia-Ramos, K. Splittorff and S. Zafeiropoulos, “The microscopic Twisted Mass Dirac spectrum and the spectral determination of the LECs of Wilson χ -PT,” PoS LATTICE **2015** (2016) 058 [arXiv:1510.09169 [hep-lat]].
 - [39] K. Cichy, E. Garcia-Ramos, K. Splittorff and S. Zafeiropoulos, “Twisted Mass Wilson χ -PT Versus Lattice Data: a Case Study,” Acta Phys. Polon. Supp. **9**, 427 (2016).
 - [40] C. Gattringer and S. Solbrig, “Remnant index theorem and low-lying eigenmodes for twisted mass fermions,” Phys. Lett. B **621**, 195 (2005) [hep-lat/0503004].
 - [41] B. Sheikholeslami and R. Wohlert, “Improved Continuum Limit Lattice Action for QCD with Wilson Fermions,” Nucl. Phys. B **259**, 572 (1985).
 - [42] K. Splittorff and J. J. M. Verbaarschot, “The Wilson Dirac Spectrum for QCD with Dynamical Quarks,” Phys. Rev. D **84**, 065031 (2011) [arXiv:1105.6229 [hep-lat]].
 - [43] J. Smit and J. C. Vink, “Remnants of the Index Theorem on the Lattice,” Nucl. Phys. B **286**, 485 (1987).
 - [44] S. Itoh, Y. Iwasaki and T. Yoshie, “The U(1) Problem and Topological Excitations on a Lattice,” Phys. Rev. D **36**, 527 (1987).
 - [45] R. G. Edwards, U. M. Heller, J. E. Kiskis and R. Narayanan, “Quark spectra, topology and random matrix theory,” Phys. Rev. Lett. **82**, 4188 (1999) [hep-th/9902117].
 - [46] R. Kaiser and H. Leutwyler, “Large N(c) in chiral perturbation theory,” Eur. Phys. J. C **17**, 623 (2000) [hep-ph/0007101].
 - [47] R. Baron *et al.*, “Light hadrons from lattice QCD with light (u,d), strange and charm dynamical quarks,” JHEP **1006**, 111 (2010) [arXiv:1004.5284 [hep-lat]].
 - [48] R. Baron *et al.* [ETM Collaboration], “Computing K and D meson masses with $N_f = 2+1+1$ twisted mass lattice QCD,” Comput. Phys. Commun. **182**, 299 (2011) [arXiv:1005.2042 [hep-lat]].

- [49] Y. Iwasaki, “Renormalization Group Analysis of Lattice Theories and Improved Lattice Action: Two-Dimensional Nonlinear $O(N)$ Sigma Model,” Nucl. Phys. B **258**, 141 (1985).
- [50] Y. Iwasaki, K. Kanaya, T. Kaneko and T. Yoshie, “Scaling in $SU(3)$ pure gauge theory with a renormalization group improved action,” Phys. Rev. D **56**, 151 (1997) [hep-lat/9610023].
- [51] R. Frezzotti and G. C. Rossi, “Twisted mass lattice QCD with mass nondegenerate quarks,” Nucl. Phys. Proc. Suppl. **128** (2004) 193 [hep-lat/0311008].
- [52] N. Carrasco *et al.* [ETM Collaboration], “Up, down, strange and charm quark masses with $N_f = 2+1+1$ twisted mass lattice QCD,” Nucl. Phys. B **887**, 19 (2014) [arXiv:1403.4504 [hep-lat]].
- [53] J. C. Osborn and J. J. M. Verbaarschot, “Thouless energy and correlations of QCD Dirac eigenvalues,” Phys. Rev. Lett. **81**, 268 (1998) [hep-ph/9807490].
- [54] M. Lüscher, “Properties and uses of the Wilson flow in lattice QCD,” JHEP **1008**, 071 (2010) [JHEP **1403**, 092 (2014)] [arXiv:1006.4518 [hep-lat]].
- [55] P. de Forcrand, M. Garcia Perez and I. O. Stamatescu, “Topology of the $SU(2)$ vacuum: A Lattice study using improved cooling,” Nucl. Phys. B **499**, 409 (1997) [hep-lat/9701012].
- [56] C. Alexandrou, A. Athenodorou and K. Jansen, “Topological charge using cooling and the gradient flow,” Phys. Rev. D **92**, no. 12, 125014 (2015) [arXiv:1509.04259 [hep-lat]].
- [57] C. Alexandrou, M. Constantinou, H. Panagopoulos [ETM Collaboration], “Renormalization functions for $N_f=2$ and $N_f=4$ Twisted Mass fermions,” arXiv:1509.00213 [hep-lat].
- [58] B. Blossier *et al.* [ETM Collaboration], “Renormalization of quark propagator, vertex functions, and twist-2 operators from twisted-mass lattice QCD at $N_f=4$,” Phys. Rev. D **91**, no. 11, 114507 (2015) [arXiv:1411.1109 [hep-lat]].
- [59] K. Cichy, E. Garcia-Ramos and K. Jansen, “Chiral condensate from the twisted mass Dirac operator spectrum,” JHEP **1310**, 175 (2013) [arXiv:1303.1954 [hep-lat]].
- [60] K. Jansen and C. Urbach, “tmLQCD: A Program suite to simulate Wilson Twisted mass Lattice QCD,” Comput. Phys. Commun. **180**, 2717 (2009) [arXiv:0905.3331 [hep-lat]].
- [61] C. Urbach, K. Jansen, A. Shindler and U. Wenger, “HMC algorithm with multiple time scale integration and mass preconditioning,” Comput. Phys. Commun. **174**, 87 (2006) [hep-lat/0506011].